ISSN (Online) 2395-2717
International Journal of Engineering Research in Electrical and Electronic Engineering (IJEREEE)
Vol 2, Issue 8, August 2016

Performance of Two Stage Inverter Based Grid Connected Photovoltaic Power Plant under Grid Faults

[1] T.J.Deepthi [2] G.Seshadri
[1] M.Tech [2] Associate Professor
Department of Electrical & Electronics Engineering,
Siddharth Institute of Engineering and Technology, Puttur-517583, Chittoor (D), Andhra Pradesh, India.

Abstract: **-- Grid-connected distributed generation sources interfaced with voltage source inverters (VSIs) need to be disconnected from the grid under: 1) excessive dc-link voltage; 2) excessive ac currents; and 3) loss of grid-voltage synchronization. In this paper, the control of two-stage grid-connected VSIs in photovoltaic (PV) power plants is developed to address the issue of inverter disconnecting under various grid faults. Inverter control incorporates reactive power support in the case of voltage sags based on the grid codes' (GCs) requirements to ride-through the faults and support the grid voltages. A case study of a 1-MW system simulated in MATLAB/Simulink software is used to illustrate the proposed control. Problems that may occur during grid faults along with associated remedies are discussed. The results presented illustrate the capability of the system to ride-through different types of grid faults.**

***Keywords*— DC–DC converter, fault-ride-through, photo- voltaic (PV) systems, power system faults, reactive power support.**

I. INTRODUCTION

FAULT STUDIES are important in large-scale grid connected renewable energy systems and have been reported in the technical literature.

However, most of these studies focused on grid-connected wind power plants [1], [2]. In the case of grid-connected photovoltaic (PV) power plants (GCPPPs), research reported thus far focused on fault-ride-through (FRT) capability [3], [4]. Spec- ifically, a three-phase current-source inverter (CSI) configuration was investigated under various fault conditions in [5] and [6], in which the out-put currents remain limited under all types of faults due to the implementation of a current-source model for the inverter. However, this configuration may lead to instability under dynamic conditions [7]. Three-phase voltage source inverters (VSIs) are used in grid-connected power conversion systems. Due to the increasing number of these systems, the control of the VSIs is required to operate and support the grid based on the grid codes (GCs) during voltage disturbances and unbalanced conditions.

Among several studies for unbalanced voltage sags, a method was introduced in [8] to mitigate the peak output currents of a 4.5-kVA PV system in non-faulty phases. Another study in[9] presented a proportional-resonant(PR) current controller for the current limiter to ensure sinusoidal output current waveforms and avoid over-current. However, in the mentioned studies, reactive power support was not considered. In [10], a study dealing with the control of the positive and negative sequences was performed. Two parallel controllers were implemented, one for each sequence. The study demonstrated the dynamic limitations of using this control configuration due to the delays produced in the current control loops. A study was reported in [11] for the control of the dc side of the inverter, which shows the impact of various types of faults on the voltage and current of the PV array.

Some of studies are based both categories can provide FRT capability; the passive methods have the drawbacks of requiring additional components and dissipating significant power during the voltage sag processes. In the application of GCPPPs with the configurations of single-stage conversion, some research was done in [18] and [19] evaluating the FRT issues of both ac and dc sides of the inverter under unbalanced voltage conditions. However, in the application of a two-stage conversion , no paper so far has proposed a comprehensive strategy to protect the inverter during voltage sags while providing reactive power support to the grid. All the designs and modifications for the inverter in both the single- and two-stage conversions have to accommodate various types of faults

ISSN (Online) 2395-2717
International Journal of Engineering Research in Electrical and Electronic Engineering (IJEREEE)
Vol 2, Issue 8, August 2016

and address FRT capability based on the GCs [20]. PV inverter disconnection under grid faults occurs due to mainly three factors: 1) excessive dc-link voltage; 2) excessive ac currents; and 3) loss of grid voltage synchronization, which may conflict with the FRT capability.

In this paper, the control strategy introduced in [18] for a single-stage conversion is used, although the voltage sag detection and reactive power control is modified based on individual measurements of the grid voltages. The main objective of this paper is to introduce new control strategies for the two-stage conversion in GCPPPs that allow the inverter to remain connected to the grid under various types of faults while injecting reactive power to meet the required GCs. Some selected simulation results for single- and two-stage configurations are presented to confirm the effectiveness of the proposed control strategies.

II.GRID CODES

As the German GCs are the most comprehensive codes for the different power levels of PV installations and integration technologies [21], this paper follows these codes as a basis for the discussions. During voltage sags, the GCPPP should sup- port the grid voltage by injecting reactive current. The amount of reactive current is determined based on the droop control defined as follows:

$$i_{qref} = droop \,|de_L|\, I'_n \quad \text{for} \quad \frac{|de_L|}{E_n} \geq 10\% \quad \text{and droop} \geq 2 \qquad \ldots\ldots\ldots\ldots\ldots\ldots\ldots\ldots\ldots\ldots\ldots\ldots\ldots\ldots(1)$$

where droop is a constant value, d_{eL} is the amount of voltage drop, and I'_n is the rated current of the PV inverter in d_q coordinates, i.e., $I'_n = \sqrt{3} I_n$, where I_n is the rated rms line current of the inverter. The amount of voltage drop d_{eL} is obtained based on the lowest rms value of the line-to-line voltages of the three phases at the terminal of the GCPPP, i.e., e_{Lmin} shown in Fig. 1. The rms voltage is obtained using the following expression:

$$e_{Lrms} = \sqrt{\frac{1}{T_\omega} \int_{t-T\omega}^{t} eL^2 dt} \quad \text{, with} \quad T_\omega = \frac{T}{2} \qquad (2)$$

Where e_L is the instantaneous line-to-line voltage, Twis the window width for the rms value calculation, and T is the grid voltage period, which is equal to 20 ms for a grid frequency of 50 Hz. The resulting control diagram for the reactive current generation is depicted in Fig. 1.

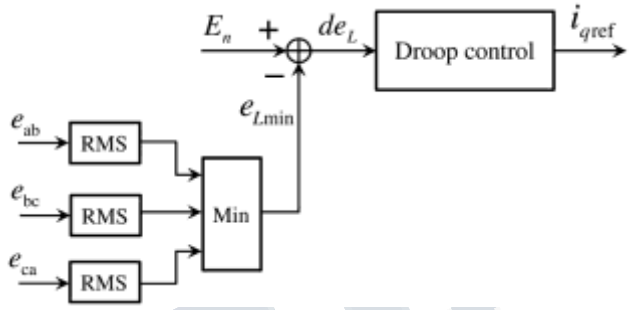

Fig. 1. Droop control diagram for the reactive current reference provision.

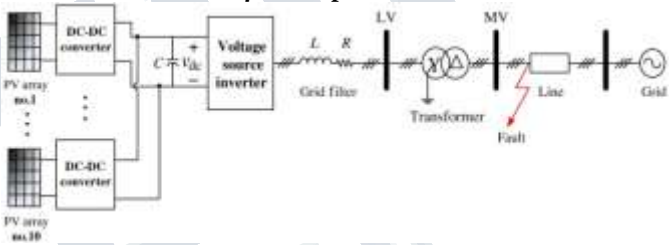

Fig. 2. Diagram of the two-stage conversion-based GCPPP

III. CASE STUDY FOR A TWO -STAGE CONVERSION

A two-stage GCPPP includes a dc–dc converter between the PV arrays and the inverter. In high-power GCPPPs, more than one dc–dc converter can be included, one per each PV array. Despite having several dc–dc converters, these systems will be referred anyway as two-stage GCPPPs. In two-stage GCPPPs, the MPP tracking (MPPT) is performed by the dc–dc converter and the dc-link voltage is regulated by the inverter.

During voltage sag, if no action is taken in the control of the dc–dc converter, the power from the PV modules is not reduced and therefore, the dc-link voltage keeps rising and may exceed the maximum limit. Hence, the system is not self-protected during grid fault conditions. A specific control action has to be taken to reduce the power generated by the PV modules and provide the two-stage GCPPP with FRT capability.

A simple method to provide dc-link overvoltage protection consists on shutting down the dc–dc converter

ISSN (Online) 2395-2717
International Journal of Engineering Research in Electrical and Electronic Engineering (IJEREEE)
Vol 2, Issue 8, August 2016

when the dc voltage rises above a certain limit. The dc–dc converter can be reactivated when the dc-link voltage is below a certain value using a hysteresis controller. In the solutions proposed in this paper, the dc-link voltage is controlled during the voltage sag process and there is no significant increase in the dc-link voltage during this transient.

The diagram of the case study for a two-stage GCPPP is shown in Fig. 2. It consists of a 1-MVA inverter and 10 parallel 100-kW dc–dc boost converters.

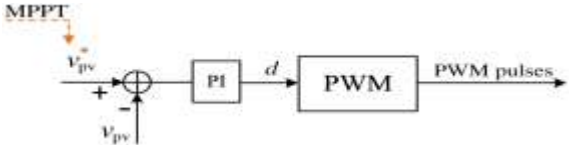

Fig 3. Control diagram of the dc–dc converter.

In two-stage GCPPPs, the PV voltage V_{pv} is controlled by the duty cycle (d) of the dc–dc converter. The reference for the PV voltage is given by the MPPT, as shown in Fig. 3.

A feed-forward strategy is applied to improve the dynamics of the dc-link voltage. The strategy is based on the assumption that the PV generated power is equal to the injected power into the grid, i.e.,

$$i_{pv}v_{pv} = e_d i_d + e_q i_q \quad \text{..... (3)}$$

Where i_{pv} and V_{pv} are the PV current and voltage, respectively, and e_d and e_q are the d and q grid voltage components extracted by the PLL. Since the PLL forces the e_q component to be zero, the estimated d current component is obtained as

$$i_{d-est} = \frac{i_{pv}V_{pv}}{e_d} \quad \text{..... (4)}$$

In two-stage GCPPPs, three different ways to limit the dc-link voltage under fault conditions are proposed: 1) short-circuiting the PV array by turning ON the switch of the dc–dc converter throughout the voltage sag duration; 2) leaving the PV array open by turning OFF the switch of the dc–dc converter; and 3) changing the control of the dc–dc converter to inject less power from the PV arrays when compared with the pre-fault operating conditions.

It should be mentioned that in all the configurations including single-stage conversion, the MPPT is disabled during the voltage sag condition and the voltage reference of pre-fault condition (V_{mpp}) is considered. Once the fault ends, the MPPT is reactivated. In the two-stage topology, the first two solutions explained next stop transferring energy from the PV arrays to the dc bus, whereas the dc bus keeps regulated at the reference value by the voltage control loop. In the third method, the MPPT is disconnected and the PV operating point moves to a lower power level to avoid overvoltage in the dc-link. Therefore, no matter the MPPT technique is voltage or current controlled and the algorithms implemented for the MPPT, the performance of the proposed methods during the voltage sag condition remains the same because the MPPT is disconnected during the voltage sag.

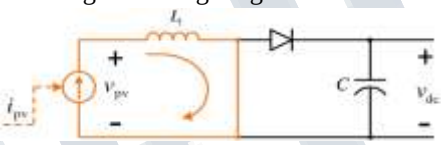

Fig 4. Current path when short-circuiting the PV panels.

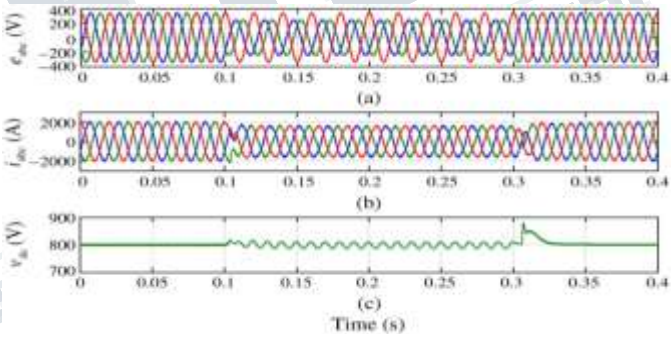

Fig. 5.Short-circuiting the PV panels: (a) grid voltages; (b) grid currents; and (c) dc-link voltage when applying a 60% SLG voltage sag at MV side of the transformer.

A. Short-Circuiting the PV Panels

In this method, the dc–dc converter switch is ON (d = 1) throughout the voltage sag, as shown in Fig. 4. Consequently, no power is transferred from the PV modules to the dc-link. Since V_{pv} is zero, the feed-forward term $i_{d\text{-}est}$ in (4) defines a fast transition to zero at the beginning of the voltage sag, accelerating the overall dynamic of the controller. Fig. 5 shows some results for an SLG voltage sag with a 60% voltage drop at MV side occurred from t = 0.1 s to t = 0.3 s. The generated power of the PV arrays and also the injected active and reactive power into the grid are shown in Fig.6. During the voltage sag, the dc-link voltage remains relatively constant, i_{ref} becomes almost zero with some ripples, and only

ISSN (Online) 2395-2717
International Journal of Engineering Research in Electrical and Electronic Engineering (IJEREEE)
Vol 2, Issue 8, August 2016

iq_{ref} is injected during the fault period. Consequently, the current limiter does not have to be activated in this case. Under unbalanced voltage sags, the output power contains a second-order harmonic [31], which will produce dc-link voltage ripples at the same frequency.

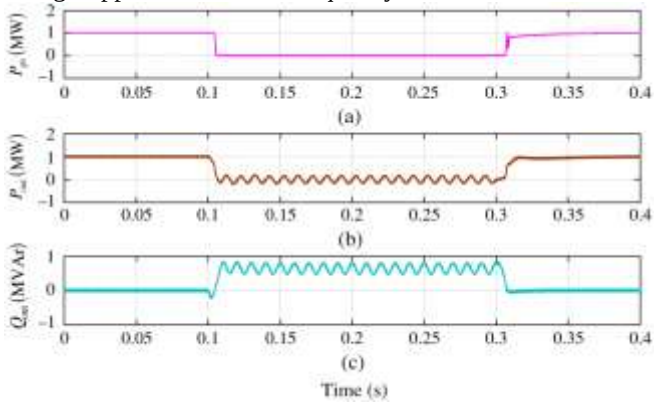

Fig.6.Short-circuiting the PVpanels: (a)overall generated power; (b) injected active power; and (c) reactive power to the grid.

B. Opening the Circuit of the PV Panels

Another option to avoid transferring power from the PV modules to the dc-link is to keep the dc–dc converter switch OFF throughout the voltage sag (d = 0), as shown in Fig. 7. Since, the inverter is not transferring active power into the grid during the voltage sag, the PV voltage V_{pv} increases until the dc–dc converter inductor is completely discharged (i_{pv}=0). Then, the diode turns OFF and the PV modules stop providing energy into the dc-link [Fig. 7(b)]. This case is similar to the previous one where the diode was continuously ON and no current from the PV was provided to the dc-link. The main difference with the previous case is the transition process, as depicted in Fig. 8.

C. Injecting Less Power From the PV Panels

In the two previous cases, during the voltage sags, there is no power generated by the PV panels and therefore, only reactive current is injected into the grid. However, as mentioned in [21], the network operator is allowed to feed the grid through the generating power plant during the voltage sags. For this purpose, the GCPPP is controlled to inject less power into the grid during the voltage sag compared with the pre-fault case, while avoiding overvoltage in the dc-link.

.

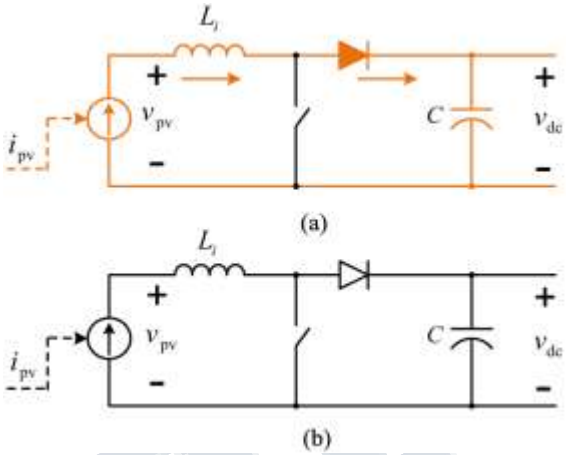

Fig.7.Current paths in dc–dc converter when turning ON the switch: (a) transition mode and (b) locked in state.

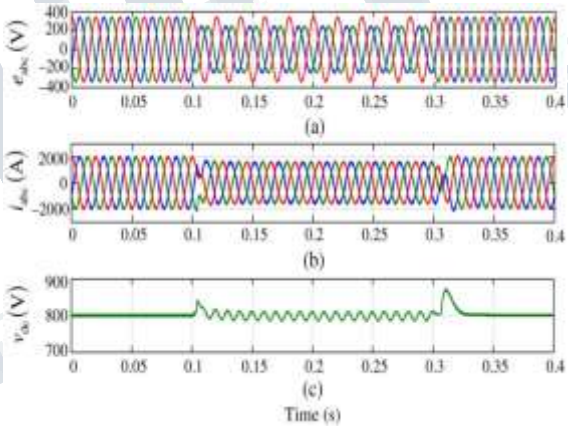

Fig. 8. Turning the dc–dc converter switch ON: (a) grid voltages; (b) grid currents; and (c) dc-link voltage when applying a 60% SLG voltage sag the MV side.

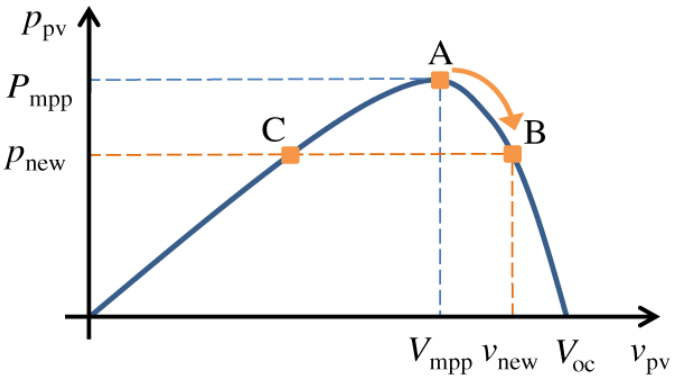

Fig 9. P−V curve and new power point under voltage sags

ISSN (Online) 2395-2717
International Journal of Engineering Research in Electrical and Electronic Engineering (IJEREEE)
Vol 2, Issue 8, August 2016

In normal operation, the MPPT function is performed by the dc–dc converter, whereas the dc-link voltage is regulated by the inverter. However, under voltage sag, some modifications should be implemented in order to keep the GCPPP grid-connected. The proposed method tries to match the power generated by the PV modules with the power injected into the grid while trying to keep the dc-link voltage constant. Unlike the previous cases of keeping the switch ON or OFF during the voltage sag, in this case, power balance is achieved for a value different from zero. Therefore, both active and reactive currents will be injected into the grid.

In the proposed method, the target of the dc–dc converter is no longer achieving MPP operation but regulating the power generated by the PVs to match the maximum active power that can be injected into the grid. The dc–dc converter is controlled to find a proper value for the PV voltage (V_{pv}) that achieves such power balance. As a result, the operating point should move from point A in Fig. 9 to a lower power point, e.g., either the points B or C. In this paper, moving the operating point in the direction from A to B is applied and analyzed. For this purpose, a positive voltage value ΔV_{pv} should be added to the V_{mpp} value that was on hold from the pre-fault situation, as follows:

$$V_{new} = V_{mpp} + \Delta_{Vpv} \quad \text{.....(5)}$$

This displacement of the operating point ΔV_{pv} is achieved by means of a PI controller that regulates the dc-link voltage to the rated value. In order to achieve a faster dynamic, the energy in the dc-link capacitor $\left(\frac{1}{2}CV_{dc}^2\right)$ is regulated instead of the dc- link voltage (V_{dc}). The schematic of this controller is shown in Fig. 10 in which the limiter is used to ensure only positive values for ΔV_{pv} in order to force the PV voltage to increase (move to the right-side of the MPP, i.e., from A to B in Fig. 9). It should be mentioned that ΔV_{pv} is added to the pre-fault value only under voltage sags and it is disconnected during normal operation of the GCPPP.

To ensure a fast dynamic response and maintaining the stability of the GCPPP, a feed-forward control strategy is proposed and applied to the dc-link control loop. For this purpose, a linear estimation is made based on the P −Vcurve shown in Fig. 9. Let us suppose the triangle represented by the vertices (P_{mpp}, V_{mpp}), (0, V_{mpp}), and (0, Voc), as depicted in Fig. 11.

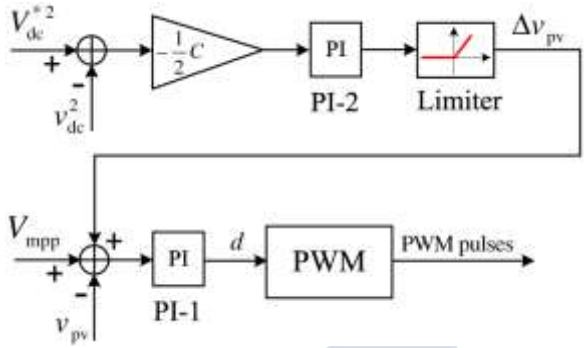

Fig. 10.Adding a controller to the dc–dc converter to force the operating point to move from the MPP to a lower power point

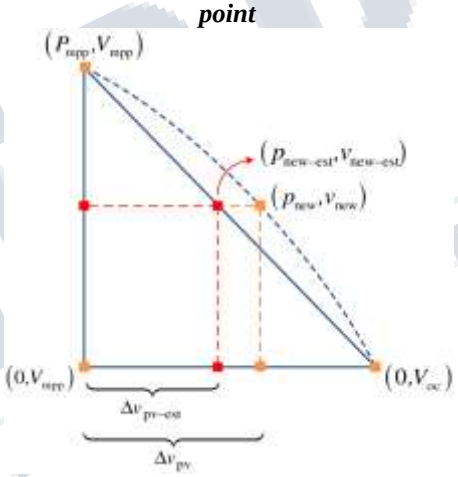

Fig. 11. Triangle used to estimate the new operating point.

The new point (P_{new} ,V_{new}) can be estimated by ($P_{new-est}$, $V_{new-est}$) on the triangle hypotenuse. According to the Side-Splitter theorem and using interpolation, the estimation of $V_{new-est}$ is

$$V_{new-est} = \frac{P_{new-est}}{P_{mpp}}\left(V_{mpp} - V_{oc}\right) + V_{oc} \quad (6)$$

in which P_{mpp} and V_{mpp} represent the pre-fault values at the MPP. The $P_{new-est}$ can be calculated from the power injected into the grid

$$P_{new-est} \cong pout = e_d\, i_{dref}. \quad (7)$$

Substituting (8) into (7)

$$V_{new-est} = \frac{e_d i_{dref}}{P_{mpp}}\left(V_{mpp} - V_{oc}\right) + V_{oc} \quad \text{.....(8)}$$

ISSN (Online) 2395-2717
International Journal of Engineering Research in Electrical and Electronic Engineering (IJEREEE)
Vol 2, Issue 8, August 2016

And

$$\Delta V_{pv-est} = V_{new-est} - V_{mpp} \quad (9)$$

The value in (9) is added to the controller as a feed-forward term before the limiter in Fig. 10, as shown in Fig. 12. In order to enhance the dynamics of the proposed controller further, another estimation can be derived using (8), which is the estimation of the duty cycle as a feed-forward term, d_{est} . Based on the relationship between the input and the output voltage of the boost dc–dc converter under continuous conduction operating conditions

$$\frac{V_{dc}}{V_{pv}} = \frac{1}{1-d} \quad (10)$$

the estimated duty cycle is

$$d_{est} = 1 - \frac{V_{new-est}}{V_{dc}^{*}} \quad (11)$$

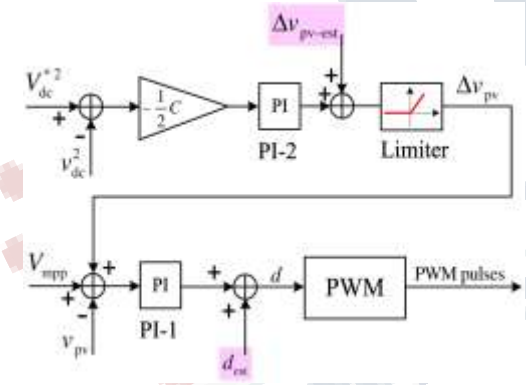

Fig. 12.Updated controller with feed-forward terms to enhance the dynamics of the proposed controller

The updated version of the controller in Fig. 10 is illustrated in Fig. 12, which contains the two feed-forward terms to enhance the dynamics of the proposed controller. The PI controllers PI-1 and PI-2 compensate for the difference between the estimated and the real values of d and ΔV_{pv} , respectively.

The only unknown variable in (8) is $i_{dref.}$ The reason is that in the proposed method, during the voltage sag, the dc-link control loop stops adjusting the active current reference and instead regulates the input voltage of the dc–dc converter (v_{pv}). The method proposed in this paper to estimate i_{dref} is the following .If Pinis the power generated by the PV array

$$P_{in} \cong e_{di'ref} + e_{q^{i}qref} \quad (12)$$

and since e_q is zero, the estimated active current reference is

$$i'_{dref-est} = \frac{P_{in}}{e_d} \quad (13)$$

The maximum acceptable value for the i_{dref} can be obtained based on the pre-fault value of Pin , i.e., P_{mpp} and e_d, as follows:

$$i'_{dref-est} = \frac{P_{mpp}}{e_d} \quad (14)$$

The estimated current $i'_{dref-est}$ goes through the current limiter and based on the required reactive current reference, i_{dref} can be obtained and substituted in (8). The performance of the proposed controller under a three-line-to-ground (3LG) with45% voltage sag at the MV side is shown in Fig. 13. As the PI controller is tuned to be slow in order to track the MPP during normal operation, the parameters of this controller (PI-1)can be increased during the voltage sag in order to improve the performance of the proposed method.

Selected results on the performance of the system under different voltage sags and different solar radiation conditions are shown in Fig. 14. As demonstrated, the output currents always remain balanced during various types of faults and solar radiations and the dynamic performance of the proposed methodtoreachthenewoperatingpointisconsiderably fast. It should be mentioned that the ripples in the dc-link voltage in Fig.14 (f)and(h) are due to the unbalanced voltage sag.

The preference of the third method, i.e., injecting less power from the PV panels, compared to the first two methods is first due to its capability to inject active power into the grid during the voltage sag to support the grid. Second, it has the capacity to inject balanced currents into the grid even under unbalanced voltage conditions. The reason is the fact that the estimated active current reference given to the current limiter is obtained based on (14), which provides an almost constant value.

ISSN (Online) 2395-2717
International Journal of Engineering Research in Electrical and Electronic Engineering (IJEREEE)
Vol 2, Issue 8, August 2016

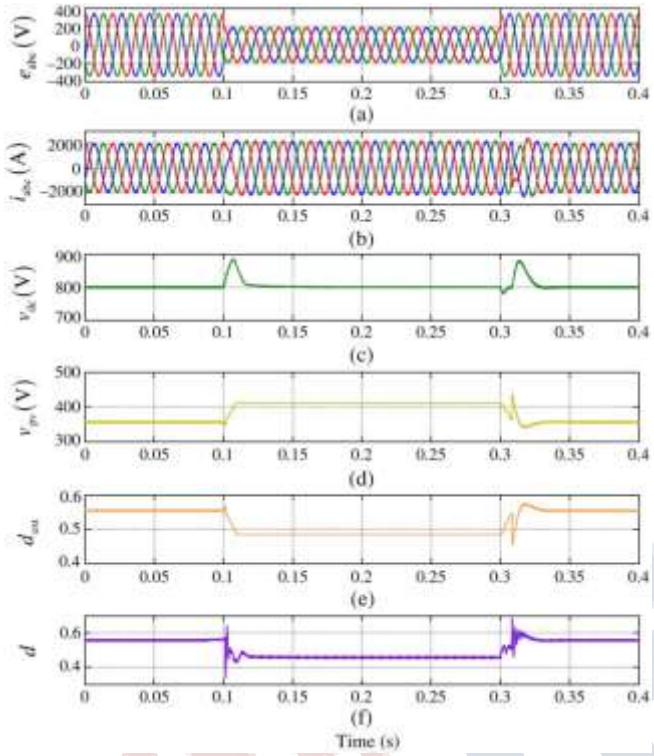

Fig. 13. Control of the dc–dc converter to produce less power under voltage sag: (a) grid voltages; (b) grid currents; (c) dc-link voltage; (d) input voltage of the dc–dc converter; (e) estimated duty cycle; and (f) actual duty cycle under a 3LG with 45% voltage sag at MV side.

IV. CONCLUSION

Performance requirements of GCPPPs under fault conditions for single- and two-stage grid-connected inverters have been addressed in this paper. Some modifications have been proposed for controllers to make the GCPPP ride-through compatible tintype of faults according to the GCs. These modifications include applying current limiters and controlling the dc-link voltage
by different methods.

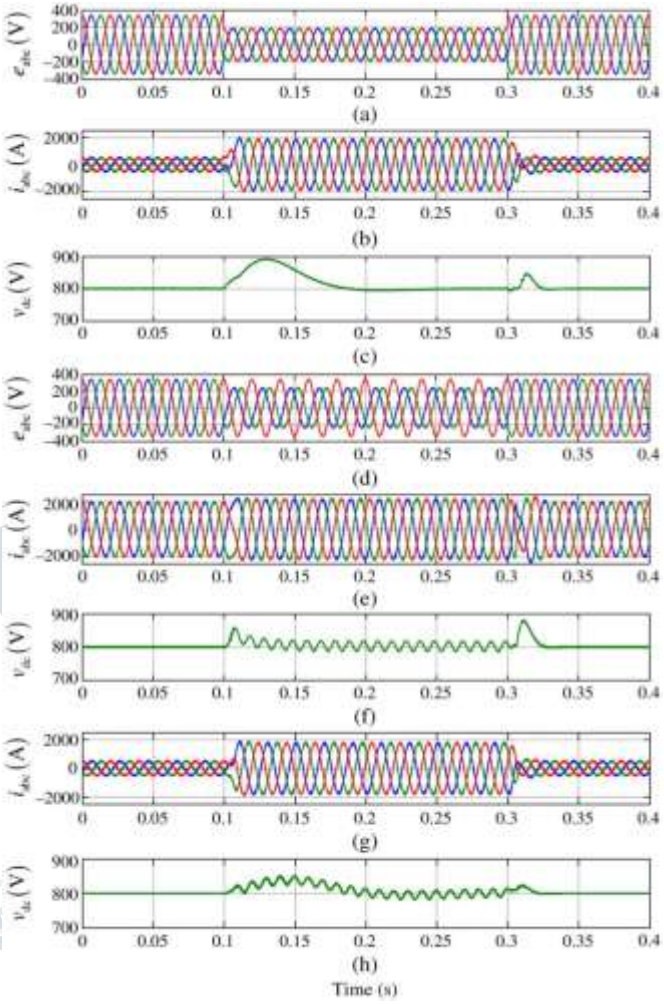

Fig. 14. Control of the dc–dc converter to produce less power under voltage sag

It is concluded that for the single-stage configuration, the dc-link voltage is naturally limited and therefore, the GCPPP is self-protected, whereas in the two-stage configuration it is not. Three methods have been proposed for the two-stage configuration to make the GCPPP able to withstand any type of faults according to the GCs with- out being disconnected. The first two methods are based on not generating any power from the PV arrays during the voltage sags, whereas the third method changes the power point of the PV arrays to inject less power into the grid compared with the pre-fault condition. The validity of all the proposed methods to ride-through voltage sags has been demonstrated by multiple case studies performed by simulations.

ISSN (Online) 2395-2717
International Journal of Engineering Research in Electrical and Electronic Engineering (IJEREEE)
Vol 2, Issue 8, August 2016

REFERENCES

[1] L. Trillaet al., "Modeling and validation of DFIG 3-MW wind turbine using field test data of balanced and unbalanced voltage sags," IEEE Trans. Sustain. Energy, vol. 2, no. 4, pp. 509–519, Oct. 2011.

[2] M. Popat, B. Wu, and N. Zargari, "Fault ride-through capability of cascaded current-source converter-based offshore wind farm," IEEE Trans. Sustain. Energy, vol. 4, no. 2, pp. 314–323, Apr. 2013.

[3] A. Marinopouloset al., "Grid integration aspects of large solar PV instal- lations: LVRT capability and reactive power/voltage support require-ments," in Proc. IEEE Trondheim PowerTech, Jun. 2011, pp. 1–8.

[4] G.Islam,A.Al-Durra, S.M.Muyeen, and J.Tamura, "Lowvoltage ride through capability enhancement of grid connected large scale photovoltaic system," in Proc. 37th Annu. Conf. IEEE Ind. Electron. Soc. (IECON), Nov. 2011, pp. 884–889.

[5] P. Dash and M. Kazerani, "Dynamic modeling and performance analysis of a grid-connected current-source inverter-based photovoltaic system,"IEEE Trans. Sustain. Energy, vol. 2, no. 4, pp. 443–450, Oct. 2011.

[6] A. Yazdaniet al., "Modeling guidelines and a benchmark for power sys- tem simulation studies of three-phase single-stage photovoltaic systems," IEEE Trans. Power Del., vol. 26, no. 2, pp. 1247–1264, Apr. 2011.

[7] A. Radwan and Y.-R.Mohamed, "Analysis and active suppression of ac- and dc-side instabilities in grid-connected current-source converter-based photovoltaic system," IEEE Trans. Sustain. Energy, vol. 4, no. 3, pp. 630–642, Jul. 2013.

[8] J. Miret, M. Castilla, A. Camacho, L. Garcia de Vicuna, and J. Matas, "Controlschemeforphotovoltaicthree-phase inverterstominimize peak currents during unbalanced grid-voltage sags," IEEE Trans. Power Electron., vol. 27, no. 10, pp. 4262–4271, Oct. 2012.

[9] G. Azevedo, P. Rodriguez, M. Cavalcanti, G. Vazquez, and F. Neves, "New control strategy to allow the photovoltaic systems operation under grid faults," in Proc. Brazilian Power Electron. Conf. (COBEP), Sep. 2009, pp. 196–201.

[10] M. Mirhosseini, J. Pou, B. Karanayil, and V. G. Agelidis, "Positive- and negative-sequence control of grid-connected photovoltaic systems under unbalanced voltage conditions," in Proc. Australasian Univ. Power Eng. Conf. (AUPEC), Sep. 2013, pp. 1–6.

[11] H. Seo, C. Kim, Y. M. Yoon, and C. Jung, "Dynamics of grid-connected photovoltaic system at fault conditions," in Proc. Transmiss. Distrib. Conf. Expo. Asia Pacific, Oct. 2009, pp. 1–4.

[12] A. Leon, J. Mauricio, and J. Solsona, "Fault ride-through enhancement of DFIG-based wind generation considering unbalanced and distorted conditions," IEEE Trans. Energy Convers., vol. 27, no. 3, pp. 775–783, Sep. 2012.

[13] D. Campos-Gaona, E. Moreno-Goytia, and O. Anaya-Lara, "Fault ride- through improvement of DFIG-WT by integrating atwo-degrees-of- freedom internal model control, in "Proc. IEEE Trans. Ind. Electron., vol. 60, no. 3, pp. 1133–1145, Mar. 2013.

[14] G. Pannell, B. Zahawi, D. Atkinson, and P. Missailidis, "Evaluation of the performance of a dc-link brake chopper as a DFIG low-voltage fault-ride- through device," IEEE Trans. Energy Convers., vol. 28, no. 3, pp. 535–542, Sep. 2013.

[15] B. Silva, C. Moreira, H. Leite, and J. Lopes, "Control strategies for ac fault ride through in multiterminal HVDC grids," IEEE Trans. Power Del., vol. 29, no. 1, pp. 395–405, Feb. 2014.

[16] I. Erlich, C. Feltes, and F. Shewarega, "Enhanced voltage drop control by VSC; HVDC systems for improving wind farm fault ridethrough capability," IEEE Trans. Power Del., vol. 29, no. 1, pp. 378–385, Feb.2014.

[17] C. Feltes, H. Wrede, F. Koch, and I. Erlich, "Enhanced fault ride-through method for wind farms connected to the grid through VSC-based HVDC transmission," IEEE Trans. Power Syst., vol. 24, no. 3, pp. 1537–1546,

ISSN (Online) 2395-2717
International Journal of Engineering Research in Electrical and Electronic Engineering (IJEREEE)
Vol 2, Issue 8, August 2016

Aug. 2009.

[18] M. Mirhosseini, J. Pou, and V. G. Agelidis, "Single-stage inverter-based grid-connected photovoltaic power plant with ride-through capability over different types of grid faults," in Proc. Annu. Conf. IEEE Ind. Electron. Soc. (IECON), Nov. 2013, pp. 8008–8013.

[19] M. Mirhosseini, J. Pou, and V. G. Agelidis, "Current improvement of a grid-connected photovoltaic system under unbalanced voltage condi- tions," in Proc. IEEE ECCE Asia Downunder (ECCE Asia), Jun. 2013, pp. 66–72.

[20] E. Troester, "New german grid codes for connecting PV systems to the medium voltage power grid," in *Proc. 2nd Int. Workshop Conc. Photovoltaic Power Plants Opt. Des. Product., Grid Connect.*, Mar. 2009, pp. 1–4.

BIOGRAPHIES

T J deepthi received B.Tech degree in Electrical and Electronics Engineering from JNTUH in 2008. Currently she is pursuing M.Tech degree in Power electronics and electrical drives at Siddharth Institute of Engineering and Technology, Puttur, India. Her Research interest in Power electronics.

G.Seshadri received B.Tech degree in Electrical and Electronics Engineering from JNTUH in 2005,M.Tech degree in Power System Operation and Control and MBA from S.V.University, Tirupathi ,India in 2008,2013 respectively and currently he is working as Associate Professor in the department of Electrical and Electronics Engineering, Siddharth Institute of Engineering and Technology, Puttur, India. His Research interest in Power systems. He is Life member of ISTE and IEEE.